

1 The authors would like to again thank the two anonymous reviewers for their further helpful
2 comments and suggestions. All comments are addressed below. Comments are included in italics
3 and author responses are in plain text.

4 Reviewer 1

5 All changes were made as suggested:

6 *line 17: saturations => saturation*

7 *line 104: "1000 nm in diameter"*

8 *line 245: α -pinene => β -pinene*

9 *line 273: resulting => substituted*

10 *para ending at 287-288: Rather than the sentence about not only 10%, I suggest simply stating that for*
11 *α -pinene, most of the nitrates would be expected to be tertiary and thus have a faster hydrolysis rate.*
12 *This is more direct, and leads nicely into the next para where you explain the mechanism.*

13 *line 329: add comma between "measurements, are"*

14

15 Reviewer 2

16 *Firstly, as the manuscript currently stands, it appears that the organic nitrates being discussed are solely*
17 *organic nitrates formed from OH+ α -pinene. However, as the authors acknowledged and agreed, that*
18 *some of the α -pinene is expected to react with ozone. The organic nitrates formed from different*
19 *oxidations (OH, ozone, NO₃) can have different hydrolysis lifetimes and fates. With this, I think it is*
20 *imperative that the authors be more upfront and make it clear throughout the manuscript that the*
21 *organic nitrates being discussed can be from OH+ α -pinene and ozone+ α -pinene.*

22 *Secondly, as the authors also acknowledged, that there are likely further reactions ongoing after the*
23 *lights are turned off (figure 3). With this, the authors need to further discuss what this implies regarding*
24 *the calculated gas-particle partitioning coefficients of organic nitrates. If there are further reactions (and*
25 *that such reactions contribute fairly substantially to the observed organic nitrates), this would introduce*
26 *large uncertainties in the concentration of the particle-phase ON and affect the values of the calculated*
27 *partitioning coefficient.*

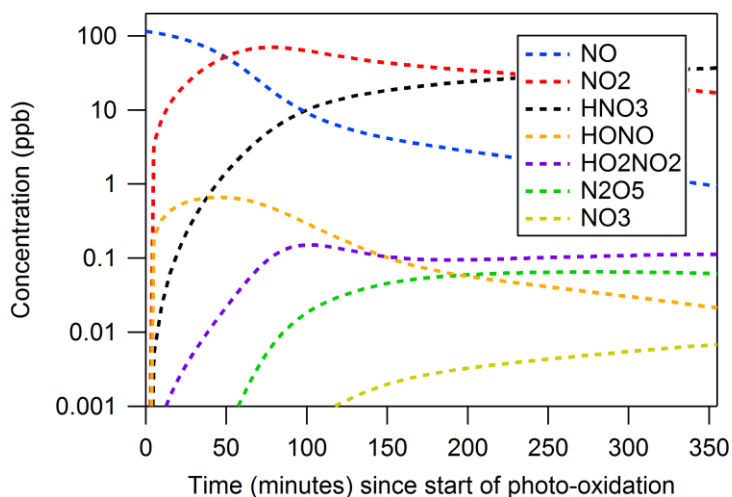
28 The responses to these comments are addressed below in the numbered responses.

29 *Please see specific comments below.*

30

31 1. Assumption that only five forms of nitrogen are present: What about HO₂NO₂? The use of H₂O₂
32 as OH precursor leads to formation of HO₂. In the presence of NO₂, does this result in the formation of
33 large amounts of HO₂NO₂?

34 We agree that HO₂NO₂ should have been included in Fig. S2. It has been added to that figure and is also
35 shown below. HO₂NO₂ concentrations are orders of magnitude lower than NO₂, NO, and HNO₃.
36 Because of this HO₂NO₂ concentrations are excluded from the mass balance calculation.



37
38 2. Uncertainties in H₂O₂ and [OH]: The authors need to include the discussions in the uncertainties
39 in the revised manuscript (i.e., as noted in their response, injection method, and chamber UV spectrum).
40 It is reasonable that if the H₂O₂ is introduced via bubbling, there will be larger uncertainties in H₂O₂ and
41 [OH]. However, I'd be quite surprised if the second method (withdrawing a known amount of H₂O₂ and
42 injecting that into the chamber with air) also introduced large uncertainties. This method has been used
43 widely in many recent laboratory chamber work, and I am not aware that this method would lead to
44 large discrepancies in estimated [OH] based on models (from H₂O₂ concentration and cross section) vs.
45 based on VOC decay. The authors noted that the model matched data for NO, NO₂, and ozone at H₂O₂
46 levels lower than those injected. How much lower? Please include this info in revised manuscript. The
47 level of H₂O₂ has direct implications on [OH] and fate of α -pinene (i.e., OH vs. ozonolysis) and possibly
48 the types of organic nitrates formed and related discussions.

49 The following paragraphs have been modified to better describe the H₂O₂ injection and estimation as
50 previously addressed in the reviewer response (updates are underlined):

51 "In these experiments only five major forms of oxidized nitrogen are present in significant
52 concentrations—NO, NO₂, HNO₃, ON^{gas} and ON^{aer} (gas and aerosol-phase organic nitrates, respectively).
53 Figure S2 shows that, based on the Statewide Air Pollution Research Center (SAPRC) model
54 (<http://www.engr.ucr.edu/~carter/SAPRC/>), the concentrations of other forms of reactive nitrogen are
55 orders of magnitude lower than the concentrations of these five forms. Concentrations of NO and NO₂
56 were measured using gas-phase monitors, ON^{aer} was measured using the ACSM, and concentrations of
57 HNO₃ were approximated using the SAPRC box model. The concentration of ON^{gas} was then calculated

58 based on a nitrogen mass balance ($ON^{gas} = NOx^{initial} - NO_2 - NO - ON^{aer} - HNO_3^{model}$), and the partitioning
59 coefficient was calculated as a time series for each experiment.”

60 The concentration of H₂O₂ used in the model was adjusted until the modeled NO, NO₂, and O₃
61 concentrations closely matched those measured throughout each experiment as shown in Fig. S3 for
62 Expt. 7. In Expts. 1, 2, and 3 (which were used to calculate the volatility basis set) H₂O₂ was injected by
63 passing air through a solution of H₂O₂ and into the chamber, and the amount of H₂O₂ injected could not
64 be estimated. In later experiments H₂O₂ was directly injected into the chamber through evaporation of a
65 known liquid volume of solution, and the estimated amount of H₂O₂ injected was about half of the H₂O₂
66 concentrations consistent with observed NO, NO₂ and O₃ based on the model. This difference may be
67 due to inefficient injection or uncertainties in the UV spectrum. The absorption cross section of H₂O₂
68 only minimally intersects with the emission spectrum of the UV lights used in this chamber. Thus, small
69 changes in the UV spectrum (or errors in measurements of the spectrum) could cause significant errors
70 in estimated concentrations of [OH], which drive the observed concentrations of NO, NO₂ and O₃.

71 3. *The authors seem to argue that it does not really matter whether α -pinene is reacting with ozone*
72 *or OH, and noted that “the interest of these experiments is the organic nitrates formed in the oxidation*
73 *of α -pinene through NO reacting with the peroxy-radical” and “ozonolysis of α -pinene is not expected to*
74 *result directly in ON”. I do not agree. Ozonolysis of α -pinene can also lead to the formation of peroxy*
75 *radicals, which can also react with NO to form organic nitrates. A recent work by Draper et al. (2015,*
76 *ACP) showed the formation of N-containing species in ozonolysis of monoterpenes in the presence of*
77 *NOx. As the reviewer pointed out earlier and the authors agreed, the relative amount of different types*
78 *of organic nitrate (e.g., primary, secondary, tertiary) can be quite different in NO₃ and OH oxidations. If*
79 *the organic nitrates discussed in this manuscript have contributions from ozonolysis (and this seems very*
80 *likely from the data presented in the manuscript), the authors need to discuss this clearly in the revised*
81 *manuscript and make the readers aware that the organic nitrates being discussed are not just organic*
82 *nitrates from OH+ α -pinene.*

83 The Reviewer is correct that while OH initiated chemistry is responsible for the bulk of the organic
84 nitrates formed, ozonolysis also plays a role. The phrase “ozonolysis of α -pinene is not expected to
85 result directly in ON” has been removed and the first paragraph of Section 3 has been updated to clarify
86 the role of ozone as follows (update underlined):

87 “A typical time series of compounds containing oxidized nitrogen is shown in Fig. 1 (Expt. 7). Initially the
88 chamber contains only NO and a small amount of NO₂, in addition to α -pinene and inorganic seed
89 aerosol. When the UV lights are activated at time = 0 the NO immediately begins to react with ·OH and
90 other radicals to form NO₂ and additional NO_y compounds such as organic nitrates. Ozone formation
91 also starts and thus in these experiments ozone also plays a role in the oxidation of α -pinene. Based on
92 the SAPRC model 15% of the total α -pinene reacts with ozone while the rest reacts with ·OH. Table 1
93 summarizes results from all experiments. Concentrations of O₃, ON^{aer}, PM organics, and ON^{gas} are
94 averaged over approximately 20 minutes of the time when PM organics and nitrates peak in
95 concentration. This averaging period was chosen so that experiments with different H₂O₂ concentrations

96 could be compared even though they reach their maximum concentrations at different rates. Higher
97 initial loading of NO_x, α-pinene, and H₂O₂ resulted in higher concentrations of ozone and PM.”

98 4. *The authors responded to my question about the uncertainty in m/z 30 (organic interference).
99 They need to include a sentence in the revised manuscript to make the readers aware of this uncertainty.*

100 This has been added to the manuscript:

101 “All PM nitrate was assumed to be organic because no inorganic nitrate was introduced in these
102 controlled experiments. PM nitrate is measured by the ACSM as NO⁺ and NO₂⁺ fragments, and the
103 standard fragmentation table is used to estimate the portion of the m/z 30 that is due to NO⁺ (as
104 opposed to (N₁₅)₂⁺ or organics).”

105 5. *Continued reaction after the lights off but before temperature increases (figure 3): The authors
106 agreed that there is continued reaction but noted that “Despite these limitations it is clear that both the
107 Org/SO₄ and ONaer/SO₄ ratios decrease with heating, consistent with semi-volatile organics and
108 organic nitrates.” I agree with this, but I also think that this can introduce large uncertainties in the
109 calculated ON partitioning coefficient and this must be made clear in the revised manuscript. In this
110 work, the partitioning coefficient is calculated from particle-ON data from ACSM and modeled gas-phase
111 ON. If the particle-ON shown in the figure has interference from other processes (i.e., continued
112 reaction), this would directly translate to large uncertainties in the partitioning coefficient. Obviously this
113 depends on the extent to which such continued reactions are occurring, but judging from the continued
114 increase in org/SO₄ after the lights are turned off (I won’t be able to tell when the lights are turned off
115 based on the data), it is clear that the contributions of these continued reactions (to org, and to ON) are
116 not small.*

117 The revised manuscript clarifies that the UV lights were on for the data used in calculating the VBS fit,
118 and that VBS parameters are static parameters used to approximate the behavior of a dynamic system.
119 (changes are underlined):

120 “Data taken throughout the lower-concentration experiments (Expts 1, 2, and 3) with UV lights on were
121 fit to a volatility basis set as these experiments were conducted under conditions which are more
122 atmospherically relevant. Volatility basis set (VBS) parameters are static but are often used to
123 approximate dynamic systems such as the one observed in these experiments. Experimental data were
124 used after total PM organics (corrected for wall losses) had reached 2 μg m⁻³ to avoid effects of noise
125 and model uncertainty at the beginning of the experiments when concentrations of both gas- and
126 particle-phase organic nitrates were low. Outlying points (for example, when PM organics temporarily
127 rose above 2 μg m⁻³ but subsequent data suggested that condensation had not begun) were removed as
128 well. Figure 5 shows the data used to find the volatility basis set along with the fit. The C* values used for
129 this were 1, 10, 100, and 1000 μg m⁻³; the corresponding mass fractions (F_i) calculated to give the best
130 fit for Eq. (2) (Sect. 2.2) are F_i = 0, 0.11, 0.03, and 0.86.”

131

132 Gas-particle Partitioning and Hydrolysis of Organic Nitrates Formed 133 from the Oxidation of α -Pinene in Environmental Chamber Experiments

134 J. K. Bean and L. Hildebrandt Ruiz

135 McKetta Department of Chemical Engineering, The University of Texas at Austin, Austin, Texas

136 Correspondence to L. Hildebrandt Ruiz (lhr@che.utexas.edu)

137 Abstract

138 Gas-particle partitioning and hydrolysis of organic nitrates (ON) influences their role as sinks and sources
139 of NO_x and their effects on the formation of tropospheric ozone and organic aerosol (OA). In this work
140 organic nitrates were formed from the photo-oxidation of α -pinene in environmental chamber
141 experiments under different conditions. Particle-phase ON hydrolysis rates consistent with observed ON
142 decay exhibited a nonlinear dependence on relative humidity (RH): An ON decay rate of 2 day^{-1} was
143 observed when the RH ranged between 20 and 60%, and no significant ON decay was observed at RH
144 lower than 20%. In experiments when the highest observed RH exceeded the deliquescence RH of the
145 ammonium sulfate seed aerosol, the particle-phase ON decay rate was as high as 7 day^{-1} and more
146 variable. The ON gas-particle partitioning is dependent on total OA concentration and temperature,
147 consistent with absorptive partitioning theory. In a volatility basis set the ON partitioning is consistent
148 with mass fractions of [0 0.11 0.03 0.86] at [saturationssaturation](#) mass concentrations (C^*) of [1 10 100
149 1000] $\mu\text{g m}^{-3}$.

150 1 Introduction

151 Organic nitrates (ON) play an important role in atmospheric chemistry as they can act as sinks and
152 sources of NO_x ($\text{NO} + \text{NO}_2$) and thereby affect the formation of tropospheric ozone and organic aerosol.
153 The sink reaction – addition of NO to a peroxy radical ($\text{R-O-O}\cdot$) to form an organic nitrate (R-O-NO_2) –
154 breaks the $\cdot\text{OH}$ initiated oxidation cycle and reduces the formation of ozone (Seinfeld and Pandis, 2006).
155 Most R-O-NO_2 molecules are semi-volatile and are therefore expected to partition between the gas and
156 particle phases. They can be transported in either phase and can become a source of NO_x when they are
157 photolyzed or oxidized, contributing to the regional nature of NO_x pollution. Attempts to implement
158 organic nitrate decomposition reactions in a chemical transport model which did not account for gas-
159 particle partitioning of organic nitrates resulted in over-prediction of NO_x and ozone concentrations
160 (Yarwood et al., 2012), consistent with an over-estimate of the strength of organic nitrates as NO_x
161 sources.

162 Recent studies have suggested that organic nitrates in the condensed phase may undergo hydrolysis,
163 leading to the formation of HNO_3 (Day et al., 2010; Darer et al., 2011; Hu et al., 2011; Liu et al., 2012;
164 Browne et al., 2013; Jacobs et al., 2014; Rindelaub et al., 2015). This is a more permanent sink for NO_x
165 and would decrease the regeneration of NO_x from organic nitrates. While these studies have found
166 evidence for hydrolysis of aerosol-phase organic nitrates (ON^{aer}), it is not clear at which rate ON

167 hydrolysis occurs. Correctly modeling organic nitrates and ozone formation depends on knowledge of
168 the ON partitioning and hydrolysis rate.

169 While ON hydrolysis in the bulk phase has been studied for decades (Baker and Easty, 1950; Baker and
170 Easty, 1952; Boschan et al., 1955), organic nitrate hydrolysis in atmospheric particles has only recently
171 started to receive attention. Day et al. (2010) observed a decrease in particulate organic nitrates
172 measured in coastal southern California under acidic conditions at high relative humidity and
173 hypothesized hydrolysis as the cause. Browne et al. (2013) used ON hydrolysis to justify observations
174 over the Boreal Forest of higher levels of HNO₃ despite higher production rates of organic nitrates. The
175 chamber experiments (0 to >80% RH) performed by Liu et al. (2012) using trimethylbenzene (an
176 anthropogenic volatile organic compound) and HONO as oxidant were the first to measure the
177 hydrolysis of condensed organic nitrates. Rindelaub et al. (2015) observed ON hydrolysis while
178 measuring partitioning of α -pinene SOA but did not directly quantify it. Boyd et al. (2015) measured
179 hydrolysis of ON formed from nitrate radical oxidation of β -pinene.

180 The partitioning of organic nitrates to the particle phase is important to determine their fate as only
181 condensed organic nitrates are expected to hydrolyze appreciably to HNO₃. Absorptive partitioning
182 theory (Pankow, 1994; Donahue et al., 2006, Rollins et al., 2013; Rindelaub et al., 2015) has been used
183 to describe the gas-particle partitioning of organic nitrates. Rollins et al. (2013) used partitioning data
184 from the 2010 CalNex Campaign to find a volatility basis set distribution for ON observed at ambient
185 aerosol concentrations. Rindelaub et al. (2015) observed the partitioning of organic nitrates formed
186 from the ·OH initiated oxidation of α -pinene at various levels of relative humidity. However, other work
187 has suggested that the partitioning of organic nitrates to the particle phase is irreversible (Perraud et al.,
188 2012). The goals of this work were to form organic nitrates in controlled environmental chamber
189 | experiments from the ·OH-initiated-dominated oxidation of α -pinene under high NO_x conditions and
190 various relative humidity levels and:

- 191 1. Quantify the hydrolysis rate of organic nitrates.
- 192 2. Confirm that the gas-particle partitioning of organic nitrates is reversible and can therefore be
193 modeled by absorptive partitioning theory
- 194 3. Parameterize the gas-particle partitioning of organic nitrates

195 **2 Methods**

196 **2.1 Environmental Chamber Experiments**

197 All experiments were performed in the Atmospheric Physicochemical Processes Laboratory Experiments
198 (APPLE) chamber located at the University of Texas at Austin (UT-Austin). The APPLE chamber is a ~12
199 m³ Teflon[®] bag suspended inside of a temperature-controlled room. The walls of the room are lined
200 with UV lights which can be used to induce photolysis reactions. The intensity of the UV lights has been
201 characterized by the photolysis rate of NO₂, which was measured to be 0.4 min⁻¹, similar to ambient NO₂
202 photolysis rates (e.g. 0.46 min⁻¹ at a zenith angle of 40°, Carter et al., 2005). Before each experiment the

203 bag was flushed for at least 12 hours with clean air from an Aadco clean air generator (Model 737-14A)
204 at a flow rate exceeding 100 liters per minute (LPM). Ammonium sulfate ((NH₄)₂SO₄) particles (Fisher
205 Scientific, 99.5%) were injected both to monitor wall loss rates (Hildebrandt et al., 2009) as well as to act
206 as seed particles onto which organic vapors can condense. Gas phase NO was injected directly into the
207 chamber from a cylinder (Airgas, 9.94 PPM ±2%) and liquid-phase α-pinene (Sigma Aldrich, 98%) was
208 injected to a glass bulb and subsequently evaporated into the chamber with a steady stream of mildly
209 heated air. H₂O₂, which photolyzes to 2·OH, was used as ·OH radical source and was either injected by
210 bubbling air through an aqueous H₂O₂ solution (Fisher Scientific, 30% weight) or by injecting H₂O₂
211 solution into a glass bulb and subsequently evaporating it into the chamber with a steady stream of
212 mildly heated air. Some experiments were performed under dry conditions (<5% relative humidity); in
213 other experiments humidity was increased by passing air through clean water and then into the
214 chamber. Experimental conditions and results are summarized in Table 1. Results are discussed in Sect.
215 3.

216 Reactions were allowed to proceed for at least 4 hours with continuous UV light. Experiments were run
217 in a batch mode with no injections or dilution after the experiment was started; the bag volume of 12
218 m³ allowed ample time for sampling. In some cases the temperature effects on gas-particle partitioning
219 were observed by increasing temperature to 40 °C in the chamber after the UV lights had been turned
220 off (see Sect. 3.2).

221

222 2.1.1 Instrumentation

223 The composition of PM₁ (particulate matter smaller than 1 micrometer in diameter) was measured using
224 an Aerosol Chemical Speciation Monitor (ACSM) from Aerodyne Research Inc. (Ng et al., 2011). In the
225 ACSM, particles are flash-vaporized on a heater at 600 °C, and the resulting gas molecules are ionized
226 using electron-impact ionization. This harsh ionization method results in fragmentation of most
227 molecules. The molecular fragments, which are measured by a quadrupole mass spectrometer, are
228 attributed to four categories—organics, nitrate, sulfate, and ammonium - using a fragmentation table
229 (Allan et al., 2004). The instrument alternates between normal sampling and sampling through a particle
230 filter, enabling subtraction of a gas-phase background. During this study the ACSM was operated at a
231 time resolution (filter/sample cycle length) of approximately 90 seconds. The size distribution of
232 particles was measured using a Scanning Electrical Mobility System (SEMS) from Brechtel
233 Manufacturing, Inc. The SEMS uses a Differential Mobility Analyzer (DMA) to size-select particles based
234 on their electric mobility, which are then counted by a Condensation Particle Counter (CPC). The DMA
235 continuously cycled between the voltages which select particles ranging from 5 to 1000 nm [in diameter](#),
236 resulting in a time resolution of the particle size distribution of approximately 60 seconds.

237 Gas phase reaction products were monitored using a High-Resolution Time-of-Flight Chemical Ionization
238 Mass Spectrometer (HR-ToF-CIMS) from Aerodyne Research, Inc.. The HR-ToF-CIMS uses softer chemical
239 ionization which results in minimal fragmentation of parent molecules. Mass spectra are derived from
240 measurements of the ions' time-of-flight as they are pulsed through a low pressure chamber in a "V"
241 shape. Two chemical reagent ions were used—water clusters (H₃O⁺·(H₂O)_n) and iodide-water clusters (I⁻

242 $\cdot(\text{H}_2\text{O})_n$). Water cluster ionization is most sensitive towards detection of moderately oxidized
243 hydrocarbons; the ability to ionize and thus sensitivity is based on the relative proton affinity between
244 the water cluster and the parent molecule (Lindinger et al., 1998). This method was used to monitor α -
245 pinene as well as early-generation oxidation products. Iodide-water cluster ionization is most sensitive
246 towards detection of more highly oxidized hydrocarbons; this method was used to observe later-
247 generation oxidation products as well as HNO_3 and H_2O_2 . In the work presented here data from the HR-
248 ToF-CIMS are only used qualitatively since, as it was later discovered, a partially clogged inlet may have
249 interfered with instrument calibration and quantitative measurements.

250 Concentrations of NO and O_3 were measured using Teledyne chemiluminescence NO_x and absorption O_3
251 monitors (200E and 400E, respectively); concentrations of NO_2 were measured via an NO_2 monitor from
252 Environnement (Model AS32M), which uses a Cavity Attenuated Phase Shift (CAPS) method to directly
253 measure NO_2 (Kebabian et al., 2008). The advantage of this direct NO_2 measurement is that it does not
254 rely on NO_2 conversion to NO and therefore does not suffer from interference by other oxidized
255 nitrogen compounds such as HONO and organic nitrates (Winer et al., 1974).

256 2.1.2 Data Analysis

257 Data from the ACSM were analyzed in Igor Pro using the software package “ACSM Local,” which includes
258 a correction for relative ion transmission efficiency as well as changes in the flow rate throughout the
259 experiment. The SEMS volume concentration was converted to mass using the densities 1.77 g/cm^3 for
260 ammonium sulfate and 1.4 g/cm^3 for organics and organic nitrates (Ng et al., 2007). The time series of
261 particle mass concentration (not corrected for wall losses) during Expt. 7 is shown in Fig. S1; other
262 experiments exhibited similar time series.

263 All PM nitrate (~~measured by the ACSM as NO^+ and NO_2^+ fragments~~) was assumed to be organic because
264 no inorganic nitrate was introduced in these controlled experiments. PM nitrate is measured by the
265 ACSM as NO^+ and NO_2^+ fragments, and the standard fragmentation table is used to estimate the portion
266 of the m/z 30 that is due to NO^+ (as opposed to $(\text{N}_{15})_2^+$ or Organics). Nitric acid is formed in the gas
267 phase as well as in the particle phase through hydrolysis, but it is assumed that nitric acid
268 concentrations are negligible in the particle phase due to its high vapor pressure (Fry et al., 2009). A
269 Henry’s Law calculation suggests that the total amount of aqueous HNO_3 in particles is 3 orders of
270 magnitude lower than that in the gas phase.

271 The ACSM does not detect all sampled particles, primarily due to particle bounce at the vaporizer,
272 resulting in a collection efficiency (CE) smaller than 1. Collection efficiency and wall losses were
273 accounted for simultaneously by multiplying the ACSM concentrations of organics and organic nitrates
274 by the mass concentration ratio $C_{SEMS}^{t=0}/C_{ACSM}^{seed}(t)$ as has been done in previous work (Hildebrandt et al.,
275 2009). Here, $C_{SEMS}^{t=0}$ is the mass concentration of ammonium sulfate seed just before the UV lights are
276 turned on and organic aerosol formation commences and $C_{ACSM}^{seed}(t)$ is the time dependent mass
277 concentration of $(\text{NH}_4)_2\text{SO}_4$ measured by the ACSM throughout the experiment. This correction assumes
278 that particles on the chamber walls participate in gas-particle partitioning as though they are still in
279 suspension and that the suspended ammonium sulfate concentration changes only due to wall losses. It

280 accounts for partitioning of organic vapors into wall-deposited particles (Hildebrandt et al., 2009) but
281 does not account for losses of organic vapors onto the clean Teflon® walls (e.g. Matsunaga and Ziemann,
282 2010).

283 The ACSM standard fragmentation table was adjusted based on filter measurements taken in each
284 experiment as described in the supplementary information. Data from the HR-ToF-CIMS were analyzed
285 in Igor Pro (Wavemetrics) using Tofware, the software provided with the instrument. The data were first
286 mass calibrated based on HR-ToF-CIMS reagent ions and other known ions. The baseline was subtracted
287 and the average peak shape was found so it could be used for high resolution analysis, through which
288 multiple ions can be identified at any given integer m/z . Ions up to m/z 300 were analyzed in high
289 resolution mode. Only prominent ions were fit above m/z 200 because of the high number of possible
290 ions at this high m/z . After ions were identified in the high resolution spectrum, the peaks were
291 integrated to yield a time series of ions. Analyte ion concentrations were then normalized by the
292 reagent ion concentrations – the sum of H_3O^+ , $\text{H}_3\text{O}^+\cdot(\text{H}_2\text{O})$ and $\text{H}_3\text{O}^+\cdot(\text{H}_2\text{O})_2$ for water cluster
293 ionization and the sum of I^- and $\text{I}^-\cdot(\text{H}_2\text{O})$ for iodide-cluster ionization. This correction accounts for
294 changes in reagent ion concentrations and instrument sensitivity during and between experiments.
295 Relative humidity can affect instrument sensitivity but this varied by less than 5% during each
296 experiment.

297 The partitioning coefficient of a species is defined as the ratio of the species concentration in the
298 particle phase to the total species concentration (gas and particle phase). For a single compound the
299 partitioning coefficient is the same whether it is on a mass or mole basis. However, for a mix of
300 compounds, such as those formed in $\cdot\text{OH}$ -initiated oxidation, the mass and mole-basis partitioning
301 coefficients will be different, with the coefficient expected higher on a mass basis since higher molecular
302 weight compounds typically have lower vapor pressure. The partitioning coefficient in this work was
303 calculated on a mole basis, in part because fragmentation in the ACSM makes it impossible to tell the
304 original size and identity of ON molecules. This mole-basis partitioning coefficient is also more useful for
305 most modeling efforts which group chemical species without knowledge of their exact molecular
306 identity. The particle-phase ON concentration was quantified using data from the ACSM: the mass
307 concentration of nitrate measured by the ACSM was converted to mixing ratio (ppb) using the molecular
308 weight of the nitrate functional group (62 g/mol). This assumes that the ON have only one nitrate
309 functional group. Conversion of the nitrate mass concentration to mixing ratio avoids the need to
310 assume an ON molecular weight (needed to estimate ON mass concentrations from ACSM) and is
311 therefore deemed to be a more accurate measure of ON from the ACSM. Quantification of all gas phase
312 ON species would necessitate calibration and identification of all ON species which is not feasible.
313 Instead, a chamber box model and nitrogen balance was employed to estimate total gas-phase ON as
314 described below.

315 **2.2 Chamber Modeling and Partitioning Coefficient**

316 In these experiments only five major forms of oxidized nitrogen are present in significant
317 concentrations— NO , NO_2 , HNO_3 , ON^{gas} and ON^{aer} (gas and aerosol-phase organic nitrates, respectively).
318 Figure S2 shows that, based on the Statewide Air Pollution Research Center (SAPRC) model
319 (<http://www.engr.ucr.edu/~carter/SAPRC/>), the concentrations of other forms of reactive nitrogen are

orders of magnitude lower than the concentrations of these five forms. Concentrations of NO and NO₂ were measured using gas-phase monitors, and ON^{aer} was measured using the ACSM. Concentrations, and concentrations of HNO₃ were approximated using the SAPRC box model. The concentration of H₂O₂ cannot be estimated from the injection method used in these experiments. Therefore, the H₂O₂ concentration used in the model was adjusted until the modeled NO, NO₂, and O₃ concentrations closely matched those observed throughout each experiment as shown in Fig. S3 for Expt. 7. The modeled HNO₃ concentration was then used with the measured NO, NO₂, and ON^{aer} to find the ON^{gas} was then calculated based on a nitrogen mass balance (ON^{gas} = NOx^{initial} - NO₂ - NO - ON^{aer} - HNO₃^{model}). The, and the partitioning coefficient was then calculated as a time series for each experiment."

The concentration of H₂O₂ used in the model was adjusted until the modeled NO, NO₂, and O₃ concentrations closely matched those measured throughout each experiment as shown in Fig. S3 for Expt. 7. In Expts. 1, 2, and 3 (which were used to calculate the volatility basis set parameters) H₂O₂ was injected by passing air through a solution of H₂O₂ and into the chamber, and the amount of H₂O₂ injected could not be estimated. In later experiments H₂O₂ was directly injected into the chamber through evaporation of a known liquid volume of solution, and the estimated amount of H₂O₂ injected was about half of the H₂O₂ concentrations consistent with observed NO, NO₂ and O₃ based on the model. This difference may be due to inefficient injection or uncertainties in the UV spectrum. The absorption cross section of H₂O₂ only minimally intersects with the emission spectrum of the UV lights used in this chamber. Thus, small changes in the UV spectrum (or errors in measurements of the spectrum) could cause significant errors in estimated concentrations of [OH], which drive the observed concentrations of NO, NO₂ and O₃.

SAPRC simulations were conducted with the reaction mechanism Carbon Bond 6 revision 2 (CB6r2), which includes organic nitrate hydrolysis through a rate estimated from a combination of the work of Liu et al. (2012) and Rollins et al. (2013) (Hildebrandt Ruiz and Yarwood, 2013). Experiments were modeled with and without organic nitrate hydrolysis to see the effect this has on the predicted ON partitioning coefficient. The overall effect of this process was small, with a maximum effect being a 5% decrease to the partitioning coefficient by removing the hydrolysis mechanism from the model. This corresponded to a 17% decrease in HNO₃, which suggests that the partitioning coefficient estimated in this work is not very sensitive to changes in the modeled HNO₃ concentrations. For the results and analysis presented here the HNO₃ concentrations were taken from CB6r2 with the inclusion of the ON hydrolysis process for experiments above 20% RH and without the hydrolysis process for experiments below 20% RH. According to absorptive partitioning theory (Pankow, 1994; Donahue et al., 2006), the gas-particle partitioning of an organic species depends on its vapor pressure and the concentration of organic material in the particle phase. The fraction of a compound i in the particle phase (Y_i) is given by (Donahue et al., 2006):

$$Y_i = \left(1 + \frac{C_i^*}{C_{OA}}\right)^{-1} \quad (1)$$

where C_{OA} is the organic aerosol concentration and C_i^{*} is the saturation mass concentration of species i (the saturation vapor pressure converted to concentration units). In the volatility basis set (VBS,

358 Donahue et al., 2006), organic species are lumped by C_i^* spaced logarithmically. This leads to an overall
359 partitioning coefficient

360
$$Y_{tot} = \sum_{i=1}^n F_i \left(1 + \frac{C_i^*}{C_{OA}}\right)^{-1} \quad (2)$$

361 (Rollins et al., 2013), where F_i is the fraction of organic species in the volatility bin described by C_i^* . In
362 this work we used measurements of C_{OA} and Y_{tot} to fit the F_i using a Matlab optimization routine. These
363 VBS parameters can be used in models to represent the gas-particle partitioning of organic nitrates and
364 account for changes in partitioning with temperature and C_{OA} .

365 **3 Results and Discussion**

366 A typical time series of compounds containing oxidized nitrogen is shown in Fig. 1 (Expt. 7). Initially the
367 chamber contains only NO and a small amount of NO₂, in addition to α -pinene and inorganic seed
368 aerosol. When the UV lights are activated at time = 0 the NO immediately begins to react with \cdot OH and
369 other radicals to form NO₂ and additional NO_y compounds such as organic nitrates. Ozone formation
370 also starts and thus in these experiments ozone also plays a role in the oxidation of α -pinene. Based on
371 the SAPRC model 15% of the total α -pinene reacts with ozone while the rest reacts with \cdot OH. Table 1
372 summarizes results from all experiments. Concentrations of O₃, ON^{aer}, PM organics, and ON^{gas} are
373 averaged over approximately 20 minutes of the time when PM organics and nitrates peak in
374 concentration. This averaging period was chosen so that experiments with different H₂O₂ concentrations
375 could be compared even though they reach their maximum concentrations at different rates. Higher
376 initial loading of NO_x, α -pinene, and H₂O₂ resulted in higher concentrations of ozone and PM.

377 Figure 2 shows time series of molecular ions identified using the HR-ToF-CIMS using water cluster
378 ("positive mode") and iodide-water cluster ("negative mode") ionization. Many compounds are
379 identified with the CIMS and a select few of the most prominent compounds were chosen for Fig. 2. In
380 short time periods after switching reagent ions the sensitivity of the HR-ToF-CIMS slowly adjusts to a
381 steady state value. Minor changes during these short time periods should be taken with caution but the
382 overall trends over the 4.5 hour experiment are useful in viewing oxidation trends. The initial data
383 collected in negative mode show that formation of organic nitrates begins immediately after oxidation
384 has started. Later in the experiment the less-oxygenated compounds observed in positive mode begin to
385 decrease while the more highly oxygenated compounds observed in negative mode continue to
386 increase, consistent with oxidation and conversion of less oxidized compounds to more highly oxidized
387 compounds continuing throughout the experiment. Highly oxidized compounds which still contain ten
388 carbon atoms (as the precursor α -pinene) begin to decrease towards the end of the experiment while
389 fragmented compounds (containing less than ten carbon atoms) continue to increase, consistent with
390 fragmentation of the carbon backbone during oxidation. Molecular weights of the gas-phase compounds
391 identified here range from 221 to 279 g mol⁻¹ and align well with the range of molecular weights
392 | estimated by Fry et al. (2009) for particle-phase organic nitrates formed from NO₃ oxidation of $\alpha\beta$ -
393 pinene (229±12 to 434±25 g mol⁻¹). Gas-phase organic nitrates identified here are therefore expected to
394 be semi-volatile and to partition significantly to the particle phase.

395 3.1 Hydrolysis of Organic Nitrates

396 Concentrations of wall-loss corrected (normalized to SO_4) PM nitrate were observed to decrease at the
397 end of most experiments. These decreases of PM nitrate are attributed to physical or chemical
398 processes in the gas and aerosol phases, and an exponential decay was fit to the data to quantify the
399 decay. The exception was experiments 1 and 3 during which production of SOA was slow (primarily due
400 to lower initial H_2O_2 and α -pinene) and continued throughout the experiment, so a decay could not be
401 observed. Examples of the decay for a humid and dry experiment are shown in Fig. S4. The decay rates
402 for each experiment are reported in Table 1 and appear to depend on relative humidity as shown in Fig.
403 3. When the RH ranged between 20 and 60%, an ON decay rate of 2 day^{-1} was observed; no significant
404 ON decay was observed at RH lower than 20%. Experiments conducted at an average RH of 67% or
405 higher can exhibit a significantly higher decay rate, probably due to effects of being near the
406 deliquescence relative humidity of the ammonium sulfate seed aerosol. In experiments 10 and 12, which
407 have decay rates well above 2 day^{-1} , the chamber was initially cooled to $20 \text{ }^\circ\text{C}$ before the UV lights were
408 turned on. Once the UV lights were activated the temperature then increased to $25 \text{ }^\circ\text{C}$ and the RH
409 settled at the values indicated in Table 1. For these experiments the RH was above 80% (the
410 deliquescence RH, DRH, of $(\text{NH}_4)_2\text{SO}_4$ for several minutes, potentially resulting in aqueous aerosol.
411 Experiment 11 also reached a relative humidity above deliquescence, yet it shows a lower nitrate loss
412 rate than Expts. 10 and 12. The ratio of organics and nitrates to sulfate (seed) particles was much lower
413 in Expt. 11 compared to Expts. 10 and 12, but whether and why this would result in a different nitrate
414 loss rate is currently unclear. The relative humidity in Expt. 4 did not reach the DRH of $(\text{NH}_4)_2\text{SO}_4$. Future
415 work should focus on the fate of ON at higher ($> 60\%$) relative humidity. The generally higher nitrate loss
416 rate at higher RH makes hydrolysis of particulate nitrate functional groups the most plausible
417 explanation for the observed decay.

418 PM organics also decreased in some experiments, but their loss rate was lower and more variable than
419 that of nitrate. Based on the work by Chuang et al. (2015) the addition of a nitrate functional group
420 decreases volatility of a compound by 2.5 orders of magnitude – slightly more than the
421 resultingsubstituted alcohol group from hydrolysis. Thus, the organic compound resulting from ON is
422 more volatile than the original organic nitrate, and as a result could partition to the gas phase, resulting
423 in a decrease in PM organics.

424 No direct observation of hydrolysis (conversion of the $-\text{ONO}_2$ group to an $-\text{OH}$ group) has been made in
425 this or previous work. The estimated hydrolysis lifetime of 12 hours (loss rate of 2 day^{-1}) for particulate
426 organic nitrates is similar to hydrolysis rates suggested by other studies under humid conditions. Liu et
427 al. (2012) observed a trend similar to that shown in Fig. 3 in chamber experiments in which ON were
428 formed from the oxidation of tri-methyl benzene using HONO as the $\cdot\text{OH}$ and NO_x source. In those
429 experiments, PM nitrate was found to have negligible loss rate below 20% RH but a lifetime of 6 hours at
430 40% RH and higher. Perring et al. (2009) estimated the lifetime of isoprene nitrates to be between 95
431 minutes and 16 hours depending on their branching ratio in isoprene $\cdot\text{OH}$ oxidation. Boyd et al. (2015)
432 measured a lifetime of 3-4.5 hours for 10% of ON formed from NO_3 oxidation of β -pinene, with a much
433 longer lifetime for the remaining 90%. This suggests that 10% of the ON functional groups were tertiary
434 with the rest being primary or secondary as those have been shown to hydrolyze much slower in the

435 bulk phase (Darer et al., 2011; Hu et al., 2011). ~~In our results hydrolysis is not limited to 10% of ON,~~
436 ~~suggesting that a higher portion is~~More tertiary ON functional groups: are expected from α -pinene than
437 β -pinene, based on the location of the double bond.

438 Similar VOC precursors such as α -pinene and β -pinene can form different fractions of primary/secondary
439 and tertiary ON. When NO_3 reacts and bonds with the terminal double bond of β -pinene, an alkyl radical
440 is formed in either a primary or tertiary position (opposite of the carbon-nitrate bond). The tertiary alkyl
441 radical is more stable, so primary organic nitrates are expected to be more abundant. The double bond
442 in α -pinene is not terminal, so the NO_3 reaction produces either a secondary or tertiary ON and alkyl
443 radical. NO_3 typically bonds with the less substituted carbon of a double bond so that a more highly
444 substituted alkyl radical is formed. The reverse is true for $\text{OH}+\text{NO}$ chemistry. In this case NO reacts with
445 the peroxy-radical to form the nitrate group. The peroxy-radical, a product of O_2 and an alkyl radical, is
446 likely to be on a more substituted carbon as this would have been the more stable alkyl radical. Thus,
447 more highly substituted ON are expected from $\text{OH} + \text{NO}_x$ than from NO_3 chemistry. This has important
448 implications for attempts to model ON and the resulting NO_x recycling.

449 As Table 1 shows experiments were conducted at varying NO_x and α -pinene concentrations, relative
450 humidity, and hydrogen peroxide ($\cdot\text{OH}$ radical source) levels, which resulted in different final
451 concentrations of PM nitrate and total OA. Liu et al. (2012) suggested that a lower PM nitrate / OA ratio
452 at higher RH could be due to ON hydrolysis. In these experiments, the correlation between the ratio of
453 PM nitrate/total OA (measured when total OA was highest) and RH was very low ($R^2 = 0.02$). Thus, based
454 on these experiments, differences in the observed final PM nitrate / OA are due to experimental
455 conditions other than relative humidity.

456 3.2 Gas-particle Partitioning of Organic Nitrates

457 In order to test the reversibility of ON partitioning the temperature of the chamber was increased after
458 OA had formed (and when the UV lights were off) in some experiments. Figure 4 shows gas and particle-
459 phase measurements taken from a representative experiment (Expt. 2). After the UV lights are turned
460 off there is a 60 minute period in which the temperature stabilizes around 15 °C. This is followed by ~90
461 minutes of heating to a final temperature of 45 °C. After this the chamber is quickly cooled back to 15
462 °C. Figure 4b shows a time series of the Org/SO_4 and $\text{ON}^{\text{aer}}/\text{SO}_4$ ratios measured by the ACSM. Sulfate
463 has a low vapor pressure and does not evaporate significantly at the temperatures investigated;
464 therefore changes in the $\text{ON}^{\text{aer}}/\text{SO}_4$ and Org/SO_4 ratios with chamber temperature can be attributed to
465 partitioning of organic nitrates and other organic species between the gas and particle phases or wall
466 losses of gas-phase species. As Fig. 4b shows, Org/SO_4 and $\text{ON}^{\text{aer}}/\text{SO}_4$ decreased with increasing
467 temperature and increased with decreasing temperature, suggesting evaporation of species at higher
468 temperatures and their re-partitioning to the particle phase at lower temperatures.

469 Figure 4c shows the effects of temperature on various compounds measured in the gas phase. Several
470 organic compounds – with and without ON functional groups - increase with increasing temperature.
471 This suggests that these compounds are present in both the gas and particle phases and evaporate at
472 higher temperature resulting in increased gas phase concentrations. As temperature is increased the
473 percent change in the concentration of gas-phase $\text{C}_{10}\text{H}_{16}\text{O}_2$ is less than the change in $\text{C}_{10}\text{H}_{16}\text{O}_4$ and the

474 percent change in the concentration of gas-phase $C_{10}H_{15}NO_4$ is less than the change in $C_{10}H_{15}NO_6$. This is
475 consistent with the more highly oxidized compounds having a lower vapor pressure and evaporating
476 less. As the temperature is decreased back to 15 °C the concentrations return to the pre-heating trends,
477 suggesting that re-condensation to the particle-phase has occurred. These observations, as well as the
478 trends seen in particle-phase measurements, are consistent with equilibrium partitioning and
479 inconsistent with the irreversible partitioning of ON recently suggested by Perraud et al. (2012).

480 Other processes may influence particle and gas concentrations of organic compounds. Continuing
481 reactions with O_3 and nitrate radicals (since O_3 and NO_2 are both present) limit the ability to stop all
482 chemical activity. This is seen in the gas phase compounds, some of which appear to be changing in
483 concentration after the UV lights are off. Despite this a clear change is seen in all compounds with a
484 temperature increase. During the cooling phase (beginning at $t = 320$ minutes) the particle phase
485 organic and nitrate concentrations do not return to the original levels. It is likely that some organic
486 compounds are lost to the walls of the Teflon chamber, especially since they reach the coldest
487 temperatures during active cooling, and thus Org/SO_4 does not return to the values seen before
488 temperature changes began. Despite these limitations it is clear that both the Org/SO_4 and ON^{aer}/SO_4
489 ratios decrease with heating, consistent with semi-volatile organics and organic nitrates.

490 Table 1 summarizes the ON partitioning coefficient averaged over approximately 20 minutes from when
491 PM organics and nitrates peak in concentration. Partitioning data is not calculated for experiments
492 above 60% RH. As discussed, these experiments had higher and less consistent nitrate decay rates which
493 may affect partitioning. In addition, the wall loss correction used here and in previous work (Hildebrandt
494 et al., 2009) assumes that particles lost to the walls still participate in partitioning as though they were
495 still in suspension. This assumption may be poor if small amounts of water condense onto the walls of
496 the chamber in these high RH experiments.

497 Data ~~from~~ taken throughout the lower-concentration experiments (Expts 1, 2, and 3) with UV lights on
498 were fit to a volatility basis set as these experiments were conducted under conditions which are more
499 atmospherically relevant. Volatility basis set (VBS) parameters are static but are often used to
500 approximate dynamic systems such as the one observed in these experiments. Experimental data were
501 used after total PM organics (corrected for wall losses) had reached $2 \mu g m^{-3}$ to avoid effects of noise
502 and model uncertainty at the beginning of the experiments when concentrations of both gas- and
503 particle-phase organic nitrates were low. Outlying points (for example, when PM organics temporarily
504 rose above $2 \mu g m^{-3}$ but subsequent data suggested that condensation had not begun) were removed as
505 well. Figure 5 shows the data used to find the volatility basis set along with the fit. The C^* values used for
506 this were 1, 10, 100, and $1000 \mu g m^{-3}$; the corresponding mass fractions (F_i) calculated to give the best
507 fit for Eq. (2) (Sect. 2.2) are $F_i = 0, 0.11, 0.03, \text{ and } 0.86$.

508 As seen in Fig. 5 these results indicate that under typical ambient conditions ($< 40 \mu g/m^3$ of OA) 5-10%
509 of organic nitrates formed from the photo-oxidation of α -pinene under high NO_x conditions are
510 expected to partition to the particle phase. This is significantly lower than the organic nitrate
511 partitioning calculated by Rollins et al. (2013) for organic nitrates measured in Bakersfield, CA during the
512 CalNex campaign in 2010. In those measurements $>30\%$ partitioning of ON was observed at organic

513 aerosol concentrations of $10 \mu\text{g}/\text{m}^3$. The difference could be attributed to differences in precursor
514 molecules and levels of oxidation. Studies have shown that high NO_x conditions can shift photochemical
515 oxidation products of terpenes towards higher volatility compounds (Wildt et al. 2014). Rollins et al.
516 determined using the SPARC model (Hilal et al., 2003) that precursor molecules (a mix of C5-C15 VOCs)
517 would need two stages of oxidative chemistry beyond the initial oxidation of the VOC to reach the point
518 when 19-28% would partition to the particle phase for a C_{OA} of $3 \mu\text{g m}^{-3}$. This may suggest that the ON
519 formed in our experiments have undergone fewer than three generations of oxidation as they are more
520 volatile than the ON measured in Bakersfield during CalNex 2010. It should also be noted that the
521 thermal dissociation-laser induced fluorescence (TD-LIF) instrument used by Rollins et al. (2013) has
522 been shown in a recent study to measure PM ON a factor of two higher than the ON measured by
523 aerosol mass spectrometers (Ayres et al., 2015) which utilize similar measurement and detection
524 techniques as the ACSM used in this work. While the reasons for this difference are unknown it would
525 result in a higher partitioning coefficient compared to the one calculated from the AMS (or ACSM) and
526 explain part of the observed difference.

527 4 Conclusions

528 Organic nitrates formed during the oxidation of α -pinene decay in the particle phase at a rate of 2 day^{-1}
529 when RH is between 20 and 60%, ~~with%;~~ no significant decay was observed below ~~an 20% RH of 20%.~~
530 During experiments when the highest observed RH exceeded the deliquescence RH of the ammonium
531 sulfate seed aerosol, the particle-phase ON decay was as high as 7 day^{-1} and more variable. The
532 dependence of observed decay rate on relative humidity suggests organic nitrate hydrolysis as the most
533 plausible explanation. The gas-particle partitioning of ON determines their potential to hydrolyze.
534 Partitioning of the ON is reversible and can be described by a volatility basis set.

535 The conversion of NO_x to organic nitrates affects local ozone production. Partitioning and hydrolysis of
536 organic nitrates affect regional concentrations of organic particulate matter and ozone. The organic
537 nitrate partitioning coefficient and hydrolysis rates from this work can be used to include these
538 processes in chemical transport models and more accurately represent the effect of organic nitrates on
539 concentrations of ozone and particulate matter.

540 5 Acknowledgements

541 -This work was ~~financed~~funded in part through a grant from the Texas Commission on Environmental
542 Quality (TCEQ), administered by The University of Texas through the Air Quality Research Program
543 (Project 12-012). The contents, findings opinions and conclusions are the work of the authors and do
544 not necessarily represent findings, opinions or conclusions of the TCEQ. The work was also
545 ~~financed~~funded in part ~~through a grant by~~with funds from the State of Texas as part of the program of
546 the Texas Air Research Center (Project 312UTA0132A). ~~The contents do not necessarily reflect the views~~
547 and policies of the sponsor nor does the mention of trade names or commercial products constitute
548 endorsement or recommendation for use.

549 6 References

550

551 Allan, J. D., Delia, A. E., Coe, H., Bower, K. N., Alfarra, M. R., Jimenez, J. L., Middlebrook, A. M., Drewnick,
552 F., Onasch, T. B., Canagaratna, M. R., Jayne, J. T. and Worsnop, D. R.: A generalised method for the
553 extraction of chemically resolved mass spectra from Aerodyne aerosol mass spectrometer data, *J.*
554 *Aerosol Sci.*, 35(7), 909–922, doi:10.1016/j.jaerosci.2004.02.007, 2004.

555 Ayres, B. R., Allen, H. M., Draper, D. C., Brown, S. S., Wild, R. J., Jimenez, J. L., Day, D. A., Campuzano-
556 Jost, P., Hu, W., de Gouw, J., Koss, A., Cohen, R. C., Duffey, K. C., Romer, P., Baumann, K., Edgerton,
557 E., Takahama, S., Thornton, J. A., Lee, B. H., Lopez-Hilfiker, F. D., Mohr, C., Goldstein, A. H., Olson, K.
558 and Fry, J. L.: Organic nitrate aerosol formation via NO_x + BVOC in the Southeastern US, *Atmos.*
559 *Chem. Phys. Discuss.*, 15(12), 16235–16272, doi:10.5194/acpd-15-16235-2015, 2015.

560 Baker, J. and Easty, D.: Hydrolysis of Organic Nitrates, *Nature*, 166(4212), 156–156,
561 doi:10.1038/166156a0, 1950.

562 Baker, J. and Easty, D.: Hydrolytic Decomposition of Esters of Nitric Acid .1. General Experimental
563 Techniques - Alkaline Hydrolysis and Neutral Solvolysis of Methyl, Ethyl, Isopropyl, and Tert-Butyl
564 Nitrates in Aqueous Alcohol, *J. Chem. Soc.*, (APR), 1193–1207, doi:10.1039/jr9520001193, 1952.

565 Boschan, R., Merrow, R. T. and Van Dolah, R. W.: The Chemistry of Nitrate Esters, *Chem. Rev.*, 55(3),
566 485–510, doi:10.1021/cr50003a001, 1955.

567 Boyd, C. M., Sanchez, J., Xu, L., Eugene, A. J., Nah, T., Tuet, W. Y., Guzman, M. I. and Ng, N. L.: Secondary
568 organic aerosol formation from the β-pinene+NO₃ system: effect of humidity and peroxy radical fate,
569 *Atmos. Chem. Phys.*, 15(13), 7497–7522, doi:10.5194/acp-15-7497-2015, 2015.

570 Browne, E. C., Min, K.-E., Wooldridge, P. J., Apel, E., Blake, D. R., Brune, W. H., Cantrell, C. A., Cubison, M.
571 J., Diskin, G. S., Jimenez, J. L., Weinheimer, A. J., Wennberg, P. O., Wisthaler, A. and Cohen, R. C.:
572 Observations of total RONO₂ over the boreal forest: NO_x sinks and HNO₃ sources, *Atmos. Chem.*
573 *Phys.*, 13(9), 4543–4562, doi:10.5194/acp-13-4543-2013, 2013.

574 Carter, W., Cockeriii, D., Fitz, D., Malkina, I., Bumiller, K., Sauer, C., Pisano, J., Bufalino, C. and Song, C.: A
575 new environmental chamber for evaluation of gas-phase chemical mechanisms and secondary
576 aerosol formation, *Atmos. Environ.*, 39(40), 7768–7788, doi:10.1016/j.atmosenv.2005.08.040, 2005.

577 Chuang, W. K. and Donahue, N. M.: A two-dimensional volatility basis set – Part 3: Prognostic modeling
578 and NO_x dependence, *Atmos. Chem. Phys. Discuss.*, 15(12), 17283–17316, doi:10.5194/acpd-15-
579 17283-2015, 2015.

580 Darer, A. I., Cole-Filipiak, N. C., O’Connor, A. E. and Elrod, M. J.: Formation and stability of
581 atmospherically relevant isoprene-derived organosulfates and organonitrates., *Environ. Sci. Technol.*,
582 45(5), 1895–902, doi:10.1021/es103797z, 2011.

583 Day, D. A., Liu, S., Russell, L. M. and Ziemann, P. J.: Organonitrate group concentrations in submicron
584 particles with high nitrate and organic fractions in coastal southern California, *Atmos. Environ.*,
585 44(16), 1970–1979, doi:10.1016/j.atmosenv.2010.02.045, 2010.

586 Donahue, N. M., Robinson, A. L., Stanier, C. O. and Pandis, S. N.: Coupled partitioning, dilution, and
587 chemical aging of semivolatile organics., *Environ. Sci. Technol.*, 40(8), 2635–43,
588 doi:10.1021/es052297c, 2006.

589 Fry, J. L., Rollins, A. W., Wooldridge, P. J., Brown, S. S., Fuchs, H. and Dub, W.: Organic nitrate and
590 secondary organic aerosol yield from NO₃ oxidation of β -pinene evaluated using a gas-phase kinetics
591 / aerosol partitioning model, *Atmos. Chem. Phys.*, 9(3), 1431–1449, 2009.

592 Hilal, S., Karickhoff, S. and Carreira, L.: Prediction of the vapor pressure boiling point, heat of
593 vaporization and diffusion coefficient of organic compounds, *QSAR Comb. Sci.*, 22(6), 565–574,
594 doi:10.1002/qsar.200330812, 2003.

595 Hildebrandt, L., Donahue, N. M. and Pandis, S. N.: High formation of secondary organic aerosol from the
596 photo-oxidation of toluene, *Atmos. Chem. Phys.*, 9(9), 2973–2986, 2009.

597 | Hildebrandt Ruiz, L. and Yarwood, G.: Interactions between Organic Aerosol and NO_y, Austin, TX.
598 Prepared for the Texas AQRP (Project 12-012), by the University of Texas at Austin, and ENVIRON
599 International Corporation, Novato, CA, available at: [http://aqrp.ceer.utexas.edu/
600 projectinfoFY12_13/12-012/12-012FinalReport.pdf](http://aqrp.ceer.utexas.edu/projectinfoFY12_13/12-012/12-012FinalReport.pdf), 2013.

601 Hildebrandt Ruiz, L., Paciga, A., Cerully, K., Nenes, A., Donahue, N. M. and Pandis, S. N.: Aging of
602 Secondary Organic Aerosol from Small Aromatic VOCs: Changes in Chemical Composition, Mass Yield,
603 Volatility and Hygroscopicity, *Atmos. Chem. Phys. Discuss.*, 14, 31441–31481, 2014.

604 Hu, K. S., Darer, A. I. and Elrod, M. J.: Thermodynamics and kinetics of the hydrolysis of atmospherically
605 relevant organonitrates and organosulfates, *Atmos. Chem. Phys.*, 11(16), 8307–8320,
606 doi:10.5194/acp-11-8307-2011, 2011.

607 Jacobs, M. I., Burke, W. J. and Elrod, M. J.: Kinetics of the reactions of isoprene-derived hydroxynitrates:
608 gas phase epoxide formation and solution phase hydrolysis, *Atmos. Chem. Phys.*, 14(17), 8933–8946,
609 doi:10.5194/acp-14-8933-2014, 2014.

610 Kebabian, P. L., Wood, E. C., Herndon, S. C. and Freedman, A.: A practical alternative to
611 chemiluminescence-based detection of nitrogen dioxide: Cavity attenuated phase shift spectroscopy,
612 *Environ. Sci. Technol.*, 42(16), 6040–6045, doi:10.1021/es703204j, 2008.

613 Lindinger, W., Hansel, A., Jordan, A. and Hansel, A.: Proton-transfer-reaction mass spectrometry (PTR –
614 MS): on-line monitoring of volatile organic compounds at pptv levels, *Chem. Soc. Rev.*, 27, 347–354,
615 1998.

616 Liu, S., Shilling, J. E., Song, C., Hiranuma, N., Zaveri, R. A. and Russell, L. M.: Hydrolysis of Organonitrate
617 Functional Groups in Aerosol Particles, *Aerosol Sci. Technol.*, 46(12), 1359–1369,
618 doi:10.1080/02786826.2012.716175, 2012.

619 Matsunaga, A. and Ziemann, P. J.: Gas-Wall Partitioning of Organic Compounds in a Teflon Film Chamber
620 and Potential Effects on Reaction Product and Aerosol Yield Measurements, *Aerosol Sci. Technol.*,
621 44(10), 881–892, doi:10.1080/02786826.2010.501044, 2010.

622 Ng, N. L., Chhabra, P. S., Chan, A. W. H., Surratt, J. D., Kroll, J. H., Kwan, A. J., McCabe, D. C., Wennberg,
623 P. O., Sorooshian, A., Murphy, S. M., Dalleska, N. F., Flagan, R. C. and Seinfeld, J. H.: Effect of NO_x
624 level on secondary organic aerosol (SOA) formation from the photooxidation of terpenes, *Atmos.*
625 *Chem. Phys. Discuss.*, 7(4), 10131–10177, doi:10.5194/acpd-7-10131-2007, 2007.

626 Ng, N. L., Herndon, S. C., Trimborn, A., Canagaratna, M. R., Croteau, P. L., Onasch, T. B., Sueper, D.,
627 Worsnop, D. R., Zhang, Q., Sun, Y. L. and Jayne, J. T.: An Aerosol Chemical Speciation Monitor (ACSM)
628 for Routine Monitoring of the Composition and Mass Concentrations of Ambient Aerosol, *Aerosol Sci.*
629 *Technol.*, 45(7), 780–794, doi:10.1080/02786826.2011.560211, 2011.

630 Pankow, J. F.: An absorption model of gas/particle partitioning of organic compounds in the
631 atmosphere, *Atmos. Environ.*, 28(2), 185–188, doi:10.1016/1352-2310(94)90093-0, 1994.

632 Perraud, V., Bruns, E. a, Ezell, M. J., Johnson, S. N., Yu, Y., Alexander, M. L., Zelenyuk, A., Imre, D., Chang,
633 W. L., Dabdub, D., Pankow, J. F. and Finlayson-Pitts, B. J.: Nonequilibrium atmospheric secondary
634 organic aerosol formation and growth., *Proc. Natl. Acad. Sci. U. S. A.*, 109(8), 2836–41,
635 doi:10.1073/pnas.1119909109, 2012.

636 Perring, A. E., Bertram, T. H., Wooldridge, P. J., Fried, A., Heikes, B. G., Dibb, J., Crouse, J. D., Wennberg,
637 P. O., Blake, N. J., Blake, D. R., Brune, W. H., Singh, H. B. and Cohen, R. C.: Airborne observations of
638 total RONO₂: new constraints on the yield and lifetime of isoprene nitrates, *Atmos. Chem. Phys.*, 9(4),
639 1451–1463, doi:10.5194/acp-9-1451-2009, 2009.

640 Rindelaub, J. D., McAvey, K. M. and Shepson, P. B.: The photochemical production of organic nitrates
641 from α -pinene and loss via acid-dependent particle phase hydrolysis, *Atmos. Environ.*, 100, 193–201,
642 doi:10.1016/j.atmosenv.2014.11.010, 2015.

643 Rollins, A. W., Pusede, S., Wooldridge, P., Min, K.-E., Gentner, D. R., Goldstein, A. H., Liu, S., Day, D. A.,
644 Russell, L. M., Rubitschun, C. L., Surratt, J. D. and Cohen, R. C.: Gas/particle partitioning of total alkyl
645 nitrates observed with TD-LIF in Bakersfield, *J. Geophys. Res. Atmos.*, 118(12), 6651–6662,
646 doi:10.1002/jgrd.50522, 2013.

647 Seinfeld, J. H. and Pandis, S. N.: *Atmospheric Chemistry and Physics*, 2nd ed., Wiley-Interscience,
648 Hoboken, 2006.

649 Wildt, J., Mentel, T. F., Kiendler-Scharr, A., Hoffmann, T., Andres, S., Ehn, M., Kleist, E., M \ddot{u} sgen, P.,
650 Rohrer, F., Rudich, Y., Springer, M., Tillmann, R. and Wahner, A.: Suppression of new particle
651 formation from monoterpene oxidation by NO_x, *Atmos. Chem. Phys.*, 14(6), 2789–2804,
652 doi:10.5194/acp-14-2789-2014, 2014.

653 Winer, A. M., Peters, J. W., Smith, J. P. and Pitts, J. N.: Response of Commercial Chemiluminescent NO-
654 NO, Analyzers to Other Nitrogen-Containing Compounds, *Environ. Sci. Technol.*, 8(13), 1118–1121,
655 doi:10.1021/es60098a004, 1973.

656

657

658
659
660
661
662
663
664
665
666
667

668 Table 1. Experimental conditions and summary of results.

| Exp | initial α - pinene (ppb) | initial NO (ppb) | RH (%) | H ₂ O ₂ conc in model (ppb) ^a | O ₃ (ppb) ^b | ON ^{aer} ($\mu\text{g}/\text{m}^3$) ^{b,c} | PM Org ($\mu\text{g}/\text{m}^3$) ^{b,c} | ON ^{gas} (ppb) ^b | Part coeff ^d | Hyd. (day ⁻¹) |
|-----|---------------------------------------|------------------------|-----------|----------------------------------------------------------------------|--------------------------------------|------------------------------------------------------------------|-------------------------------------------------------|-----------------------------------------|----------------------------|------------------------------|
| 1 | 40 | 30 | 22 | 100 | 90 | 7 | 90 | 13 | 0.19 | NA ^e |
| 2 | 40 | 40 | 39 | 60 | 50 | 6 | 60 | 11 | 0.18 | 2.2 |
| 3 | 40 | 40 | 0 | 40 | 50 | 4 | 30 | 13 | 0.10 | NA ^e |
| 4 | 130 | 110 | 68 | 600 | 210 | 150 | 1700 | | | 2.4 |
| 5 | 130 | 130 | 22 | 900 | 330 | 70 | 780 | 57 | 0.33 | 1.8 |
| 6 | 130 | 120 | 50 | 500 | 240 | 40 | 460 | 47 | 0.26 | 1.9 |
| 7 | 130 | 120 | 15 | 200 | 210 | 50 | 510 | 34 | 0.38 | 0.2 |
| 8 | 80 | 80 | 0 | 1000 | 300 | 30 | 310 | 32 | 0.26 | 0.6 |
| 9 | 80 | 80 | 0 | 1500 | 330 | 20 | 270 | 28 | 0.25 | 0.2 |
| 10 | 50 | 50 | 70 | 600 | 180 | 20 | 220 | | | 6.9 |
| 11 | 40 | 40 | 70 | 200 | 70 | 10 | 70 | | | 2.5 |
| 12 | 50 | 50 | 67 | 500 | 170 | 170 | 2200 | | | 5.2 |

669 ^a H₂O₂ concentration for which SAPRC model most closely matched measurements of NO_x and O₃

670 ^b Measured and averaged over a 20 minutes period when PM organics peaked

671 ^c Corrected for wall-losses as described in Sect. 2.1.2

672 ^d Molar basis

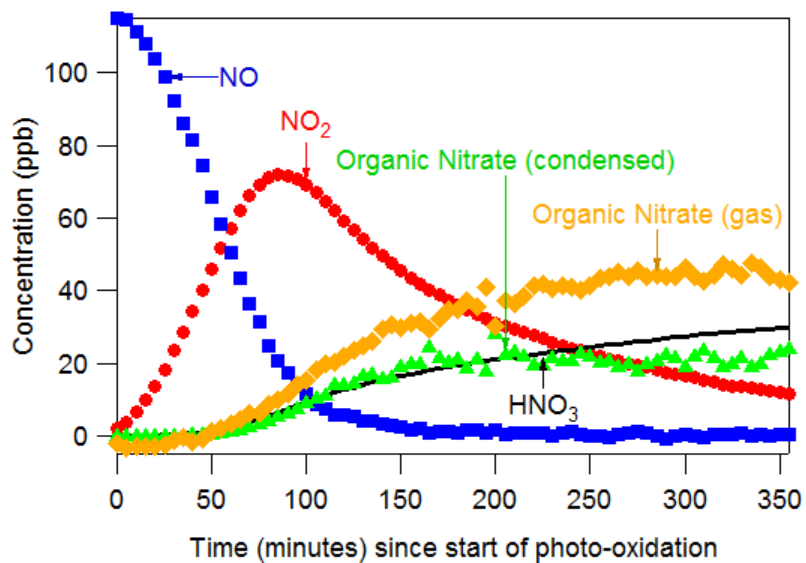
673 ^e Experimental conditions resulted in aerosol growth throughout the experiment

674
675

676

677

678



679

680 Figure 1 – Time series of oxidized-nitrogen species in Expt. 7. NO, NO₂, and ON^{aer} are measured directly.

681 HNO₃ is modeled using SAPRC. ON^{gas} is calculated from a mass balance.

682

683

684

685

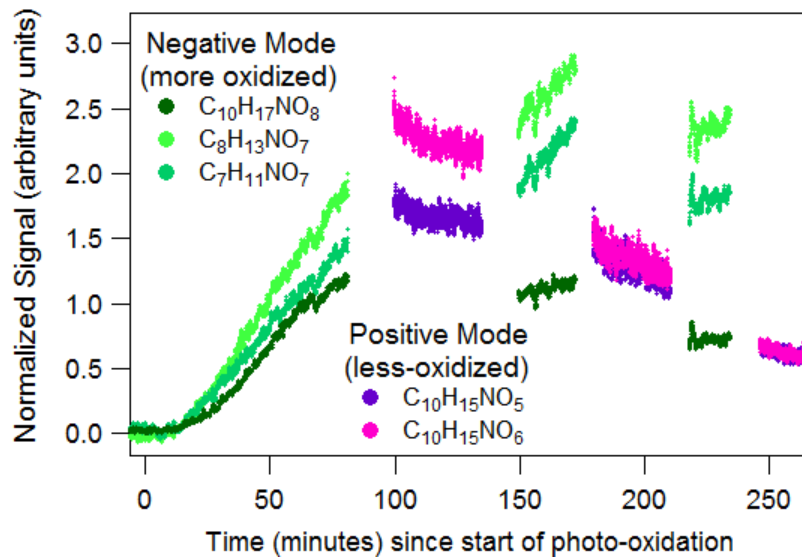
686

687

688

689

690



691

692

Figure 2 – Time series of selected organic nitrates identified by HR-ToF-CIMS (Expt. 10)

693

694

695

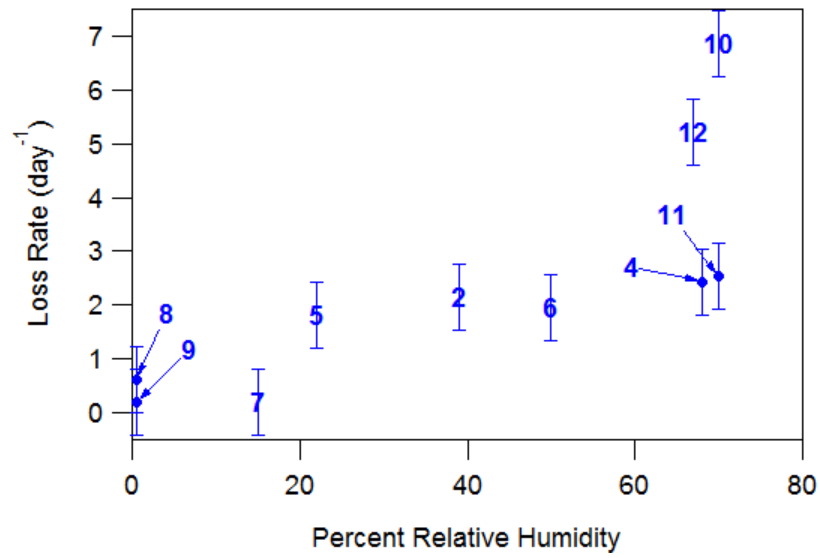
696

697

698

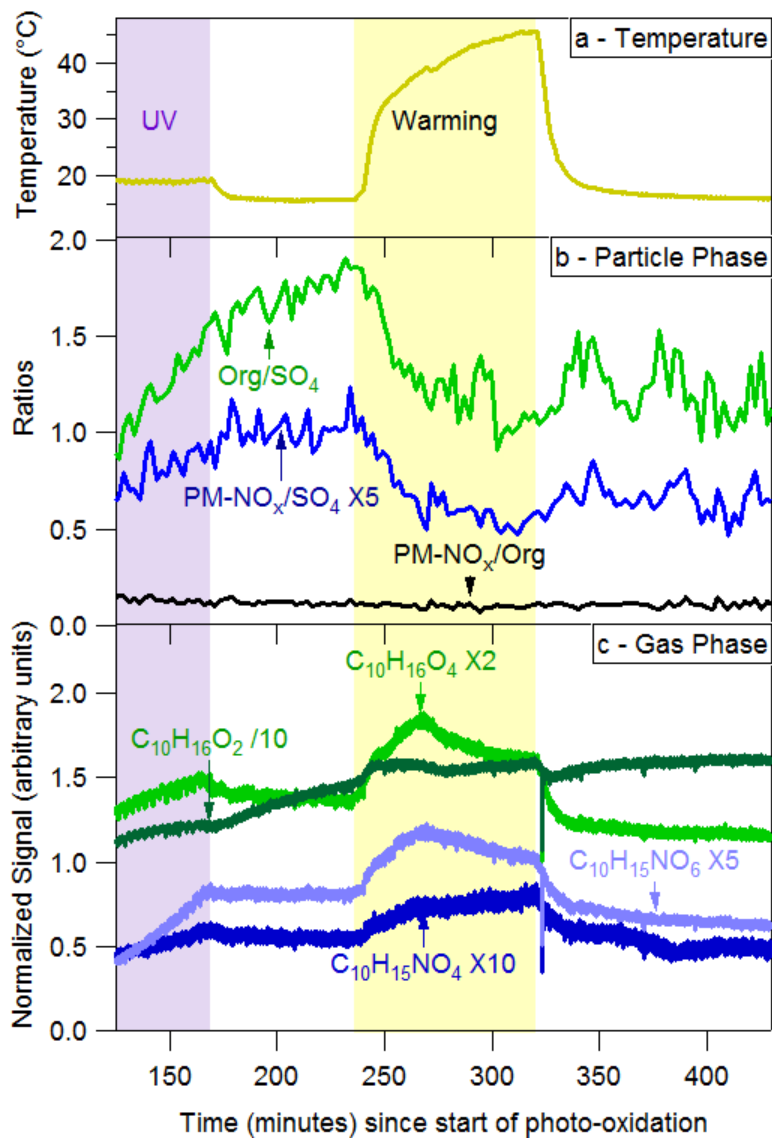
699

700



701

702 Figure 3. The organic nitrate loss rate as a function of relative humidity for Expts. 2, 4-12. Uncertainty
 703 (error bars) is estimated as 0.6 day⁻¹, the highest loss rate observed in experiments below 5% RH (Expt.
 704 8).

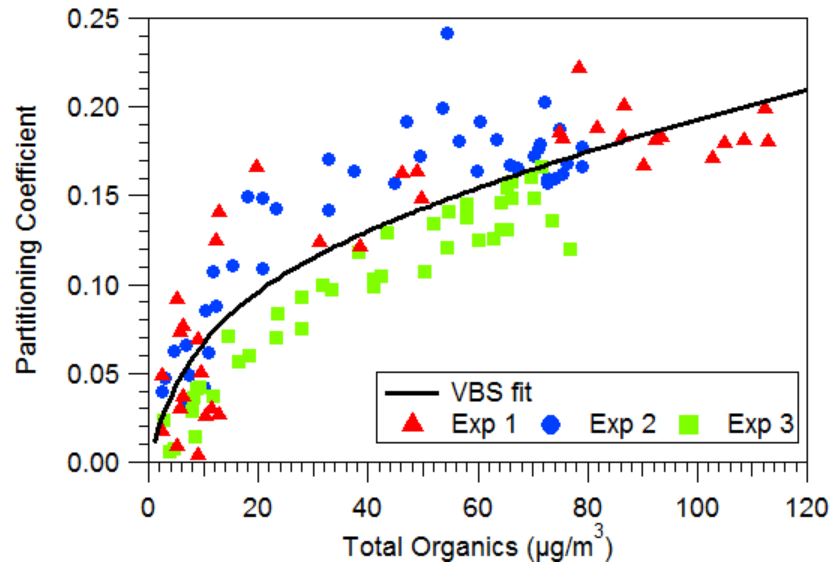


705

706

Figure 4 – Temperature effects on gas-particle partitioning of organic nitrates (Expt. 2).

707



708

709

Figure 5 – Volatility basis set fit from this work shown with data from Expts. 1, 2, and 3.

710

711